The source-lens clustering effect in the context of lensing tomography and its self-calibration

Yu Yu,[1,*] Pengjie Zhang,[2,1,†] Weipeng Lin,[1,2] and Weiguang Cui[3,4]

[1] *Key laboratory for research in galaxies and cosmology, Shanghai Astronomical Observatory, Chinese Academy of Science, 80 Nandan Road, Shanghai, China, 200030*

[2] *Center for Astronomy and Astrophysics, Department of Physics and Astronomy, Shanghai Jiao Tong University, 955 Jianchuan road, Shanghai, 200240*

[3] *ICRAR, University of Western Australia, 35 Stirling Highway, Crawley, Western Australia 6009, Australia*

[4] *ARC Centre of Excellence for All-Sky Astrophysics (CAASTRO)*

arXiv:1402.7144v1 [astro-ph.CO] 28 Feb 2014

Sampling the cosmic shear field through observation is inevitably biased, since cosmic shear can only be measured where there are galaxies and the galaxy distribution is correlated with the lensing signal. This source-lens clustering (SLC) effect has two sources, the intrinsic source clustering and the cosmic magnification (magnification/size bias). The former decreases with decreasing width of the source galaxy redshift distribution, so lensing tomography with finite source redshift bin size can suppress it. However, due to photometric redshift errors and non-zero width of redshift bins, this reduction in SLC is limited. Hence it remains unclear whether the residual can be controlled below the statistical error of stage IV lensing surveys. Furthermore, the SLC induced by the cosmic magnification can not be reduced by lensing tomography. Through N-body simulations, we quantify the impact of SLC on the lensing E/B-mode power spectrum in the context of lensing tomography. We consider two favorite estimators in measuring the lensing power spectrum, the standard estimator and the pixel-based estimator. We find that none of the two estimators can satisfactorily handle both sources of SLC. (1) For the standard estimator, the SLC induced by both the two sources can bias the lensing power spectrum by $\mathcal{O}(1\%)$-$\mathcal{O}(10\%)$ and the exact value depends on the galaxy bias and the flux/size of source galaxies. The SLC induced by the intrinsic source clustering also increases statistical uncertainties in the measured lensing power spectrum. However, the standard estimator suppresses the intrinsic source clustering induced SLC in cross power spectrum. (2) In contrast, the pixel-based estimator is efficient to suppress the SLC induced by the cosmic magnification. However, it fails to suppress the SLC induced by the intrinsic source clustering and the measured lensing power spectrum can be biased low by $\mathcal{O}(1\%)$-$\mathcal{O}(10\%)$. In a word, for typical photometric redshift error ($\sigma_z/(1+z)=0.05$) and photometric redshift bin size ($\Delta z^P=0.2$), SLC alters the lensing E-mode power spectrum by 1%-10%, at $\ell\sim10^3$ and $z_s\sim1$ of particular interest to weak lensing cosmology. We conclude that the SLC effect is a severe systematic error for weak lensing cosmology, even with the aid of lensing tomography. We present useful scaling relations to self-calibrate the SLC effect.

PACS numbers:

I. INTRODUCTION

Weak gravitational lensing — a powerful probe of the dark universe [1–6] — still suffers from many systematic errors. Ongoing lensing surveys like the dark energy survey (DES) [31] and upcoming surveys such as Euclid, LSST [32], and Subaru-HSC will achieve 1% level or better statistical precision. This puts stringent requirements on the accuracy of observational measurement and theoretical modeling [7].

There are various known systematic errors $\sim1\%$ level in weak lensing measurement (e.g. [6] and references therein), including point spread function, photometric redshift errors and galaxy intrinsic alignment. This motivates highly intensive and comprehensive efforts to understand and calibrate these systematic errors (e.g. [8]). Meanwhile, there are various sources of systematic errors in theoretical calculation of weak lensing. (1) The standard treatment adopts the Born approximation. Hence two systematic errors, Born correction and lens-lens coupling [9–12], arise. It also approximates the measured reduced shear $g\equiv\gamma/(1+\kappa)$ as γ [9, 11, 12]. (2) The standard treatment neglects the baryon effect on the evolution of the matter density distribution. Studies [13–17] show that baryons can affect the weak lensing power spectrum by $\sim1\%$ at scales of interest ($\ell\sim10^3$). (3) It also ignores various selection biases such as the source-lens clustering (SLC). This paper aims to quantify SLC in the context of lensing tomography of typical photometric redshift bin size $\Delta z^P=0.2$.

The SLC effect [18, 19] arises from the fact that we can only measure cosmic shear where there are (source) galaxies. Any spatial correlation between the distribution of source galaxies and the lens field (source-lens clustering) can lead to bias in sampling the lensing field and hence lead to biased measurement of lensing statistics. There are two known sources causing such spatial correlation. (1) One is the overlapping of source redshift distribution and lens redshift distribution. It causes spatial

*Electronic address: yuyu22@shao.ac.cn

†Electronic address: zhangpj@sjtu.edu.cn

correlation between the *intrinsic galaxy clustering* and the underlying matter (lens) distribution in the overlapping region [18]. Such overlapping is inevitable in reality. We need sufficiently wide redshift bin with sufficient amount of source galaxies to suppress shape measurement noise. For source galaxies in real redshift range of $z_1 < z_s < z_2$, lenses distribute in the range $0 < z_L < z_2$. So sources and lenses overlap at $[z_1, z_2]$. This overlap causes the intrinsic clustering of source galaxies (δ_g) to be correlated with their cosmic shear $\gamma_{1,2}$ and convergence κ, for both tracing the underlying matter distribution. This correlation leads to biased sampling of the lensing field. Photometric redshift errors further broaden the galaxy distribution in redshift, making the situation worse. (2) The other is the magnification bias [19, 22], size bias [23] or any other selection effects depending on the lensing field. For brevity we refer it as cosmic magnification. Lensing changes the galaxy flux/size and hence alters the galaxy number density, $\delta_g \to \delta_g + g\kappa$. Here, g is a function of galaxy flux and size. It ($g\kappa$) is perfectly correlated with the lensing field (κ). So this effect persists even for source redshift distribution of infinitesimal width.

Impacts of SLC on various weak lensing statistics have been investigated [18–24]. Bernardeau [18] showed that SLC by the galaxy intrinsic clustering alters lensing skewness and kurtosis at leading order. Hamana [19] extended the investigation of skewness to a wide variety of redshift distributions and bias parameters. Hamana *et al.* [20] studied SLC by the cosmic magnification (magnification bias) using semi-analytical approach. He found that lensing magnification can affect the convergence skewness by $\lesssim 3\%$. Schneider *et al.* [21] pointed out that intrinsic source clustering can produce B-mode and presented estimation based on analytical approach. Forero-Romero *et al.* [22] presented a tool coupling N-body simulations to a semi-analytical model of galaxy formation to perform mock weak lensing measurements, and studied the intrinsic source clustering effect on the probability density distribution (PDF), variance, skewness and kurtosis of the convergence. They found that σ_8 can be biased by 2%-5%. Schmidt *et al.* [23] worked on the effect of magnification and size bias on the estimation of shear correlation function. They concluded that this lensing bias should be taken seriously. This work extended the investigation to 2-point correlation function/power spectrum, compared to the previous works [19, 20] on 1-point variance and skewness. Valageas [24] adopted hierarchical ansatz and semi-analytic model to estimate the bias caused by the intrinsic source clustering on weak lensing 2-point and 3-point estimators.

Further investigations are still required to fully quantify the impact of SLC on weak lensing modeling and weak lensing cosmology. (1) Most existing works do not focus on SLC in the context of lensing tomography with realistic width of source redshift. These works either study SLC for flux-limited source galaxies with wide redshift distribution (e.g. [18–22]) or for fixed source redshift (e.g. [23, 24]). The impact of SLC for more realistic situation should fall somewhere between the two extreme cases. The SLC caused by the intrinsic source clustering increases with the source redshift width, since the cross correlation between the source galaxy distribution and the lens distribution increases with the source redshift width. So this kind of SLC effect can be reduced by lensing tomography with finite redshift width. Indeed, in the limit of infinitesimal source redshift width, the SLC effect caused by the intrinsic source clustering can be completely eliminated by the standard estimator [23]. However, photo-z errors and finite galaxy number density prohibit the real redshift width to be smaller than ~ 0.2. A question to address is then whether in this more realistic situation lensing tomography can suppress the SLC effect to a level negligible. (2) Most existing works calculate SLC approximately. Approximations made include Taylor expanding the cosmic shear estimator and approximations in evaluating high order density correlations. An exception is [22], which analyzed SLC through N-body simulations and hence avoided these uncertainties. But [22] only considered the pixel-based estimator, only on 1-point statistics (PDF, variance, etc.), and only for flux-limited galaxies. To make the investigation complete, another estimator (the standard estimator) should also be studied. (3) Given clear evidences that SLC can not be neglected for precision lensing cosmology, an immediate task is to calibrate this effect. For this purpose we shall quantify its dependence on galaxy bias or the factor g in magnification/size bias in this paper. We find useful scaling relations to correct for the SLC effect.

We will then study the SLC effect through N-body simulation, for photo-z bins of width $\Delta z^P = 0.2$. We will consider both sources of SLC, the intrinsic source clustering and the cosmic magnification. Furthermore, we will consider two popular estimators of shear correlation function/power spectrum. (1) The standard estimator. Cosmic shear is decomposed into the tangential and cross component for each galaxy pair. Then it sums over the two products of shear components over all pairs of fixed angular separation and normalizes by the number of pairs to obtain the two point statistics of cosmic shear. This standard estimator is widely used in weak lensing surveys. (2) The pixel-based estimator. It constructs shear maps by averaging over all shears in each pixel. One then performs the E-B decomposition and measures the 2-point statistics from these maps. This estimator is convenient for map-making, one point statistics such as peak statistics and PDF, or high order statistics. The two estimators differ in the order of normalization over the galaxy number density and averaging over galaxy pairs. However, none of them can satisfactorily handle both sources of SLC. Fortunately we find that there exist excellent scaling relations between SLC and observables, which allow for self-calibrating the SLC effect.

Our paper is organized as follows. The SLC effect is described in §II for both the standard estimator and the pixel-based estimator. We introduce the way we estimate

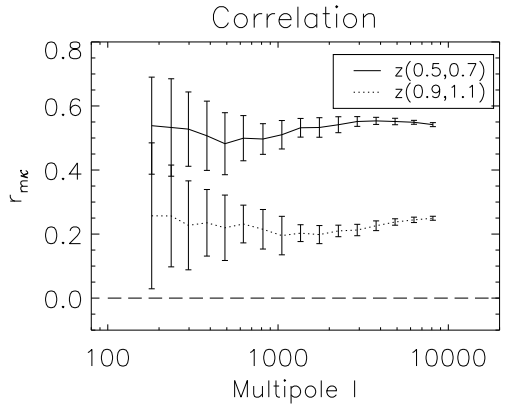

FIG. 1: Cross correlation coefficient $r_{m\kappa}$ between the source galaxy intrinsic distribution ($b_g = 1$) and the lensing signal. The error bars are the rms dispersion among 20 realizations. In the limit $\sigma_P \to 0$ and $\Delta z^P \to 0$, $r_{m\kappa} \to 0$. But for more realistic cases shown ($\Delta z^P = 0.2$ and $\sigma_P = 0.05(1+z)$), $r_{m\kappa} \sim$ 0.2-0.6 at $\ell \sim 1000$, meaning significant spatial correlation between the source galaxies and the lenses. This implies a significant SLC effect, as verified later in the paper. Increasing r with decrease reshift implies stronger SLC at lower redshift, again verified later in the paper. Notice that this is just one source of SLC. The other source is the cosmic magnification, which is always perfectly correlated with the lensing signal and lensing tomography does not help handle it.

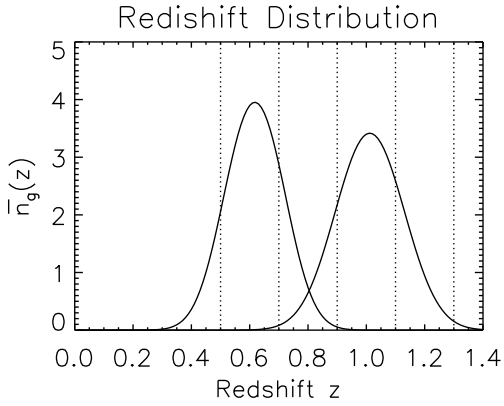

FIG. 2: The real source galaxy distribution $\bar{n}_g(z)$ of photo-z bins $(0.5, 0.7)$ and $(0.9, 1.1)$ are presented. $\bar{n}_g(z)$ is normalized to $\int \bar{n}_g(z)\mathrm{d}z = 1$. Photo-z error broadens the reshift distribution significantly, and hence increases the SLC effect.

the SLC effect through simulation in §III. The results are presented in §IV & V for the standard estimator and the pixel-based estimator, respectively. We discuss and conclude in §VI.

II. THE SLC EFFECT

Weak lensing cosmology prefers volume weighted lensing measurement. However, in reality we can measure cosmic shear γ only where there are galaxies. Thus the measured shear field is inevitably weighted by some function of n_g, the number density of observed source galaxies. The galaxy distribution fluctuates spatially, $n_g = \bar{n}_g(1 + \delta_g^{\rm obs})$. The limit of no correlation between $\delta_g^{\rm obs}$ and the lensing field corresponds to randomly sampling the lensing field. This is a fair sampling process and does not bias the measured lensing statistics. *Unfortunately, in reality $\delta_g^{\rm obs}$ correlates with the lensing field.* So the lensing field is not fairly sampled observationally. Hence this source-lens clustering (SLC) effect biases the lensing measurement.

The observed source galaxy number overdensity $\delta_g^{\rm obs}$, to leading order, has two components.

$$\delta_g^{\rm obs} = \delta_g + g\kappa \ . \tag{1}$$

Here, δ_g is the intrinsic fluctuation (intrinsic clustering). Throughout the paper we adopt a simple bias model for $\delta_g = b_g\delta_m$ where δ_m is the matter overdensity and b_g is the galaxy bias. Unless otherwise specified, we adopt $b_g = 1$. $g\kappa$ is that induced by the cosmic magnification. It arises from the thresholds in selecting galaxies, either by flux (magnification bias) or size (size bias).

Since SLC arises from $\delta_g^{\rm obs}$-κ (γ) correlation, its strength increases with the cross correlation coefficient $r_{\rm SL}$ between the two. Here the subscript "SL" denotes "source-lens".

$$r_{\rm SL}(\ell) = \begin{cases} \frac{C_{g\kappa}(\ell)}{\sqrt{C_{gg}(\ell)C_{\kappa\kappa}(\ell)}} \ , & \text{intrinsic source clustering} \\ 1 \ , & \text{cosmic magnification} \ . \end{cases} \tag{2}$$

For the intrinsic source clustering,

$$\frac{C_{g\kappa}(\ell)}{\sqrt{C_{gg}(\ell)C_{\kappa\kappa}(\ell)}} \simeq \frac{C_{m\kappa}(\ell)}{\sqrt{C_{mm}(\ell)C_{\kappa\kappa}(\ell)}} \equiv r_{m\kappa}(\ell) \ . \tag{3}$$

Here $C_{g\kappa}$, C_{gg} and $C_{\kappa\kappa}$ are the cross- and auto-power spectrum between the source galaxy angular distribution and the lensing convergence of these galaxies. $C_{m\kappa} \equiv C_{g\kappa}(b_g = 1)$. $C_{mm} \equiv C_{gg}(b_g = 1)$.

In Fig. 1, we plot $r_{m\kappa}$ measured through simulation, for two typical photo-z bins, $0.5 < z^P < 0.7$ and $0.9 < z^P < 1.1$. We adopt a source distribution

$$n^P(z^P)\mathrm{d}z^P = \frac{1}{2}\frac{z^P}{z_0^3}\exp(-\frac{z^P}{z_0})\mathrm{d}z^P \tag{4}$$

with $z_0 = 0.45$ and Gaussian photo-z error $\sigma_P = 0.05(1+z)$, typical for LSST-like surveys. The real redshift distribution is shown in Fig. 2. Photo-z errors broaden the redshift distribution and cause substantial overlap between the source and lens distribution. This results in a significant $r_{m\kappa} \sim$ 0.2-0.6 at $100 \lesssim \ell \lesssim 10^4$. The correlation strength is stronger towards lower redshift, because of the stronger redshift dependence of lensing kernel. This result directly indicates larger SLC effect

due to the intrinsic source clustering towards lower redshift [33]. The correlation coefficient only shows weak dependence on the scale, indicating that the SLC effect can be important at all scales.

Narrowing the photo-z bin reduces $r_{m\kappa}$. But this reduction is very mild, because the redshift width is $\sim 2\sigma_P \sim 0.2$ even in the limit $\Delta z^P = 0$. Hence even with the aid of photo-z information, SLC induced by the intrinsic source clustering can not be significantly reduced. We then expect non-negligible SLC even in the context of lensing tomography. Through N-body simulation, we can construct 2D maps of source and lens distribution and robustly quantify the SLC effect.

The exact impact of SLC on lensing statistics depends on the estimator of these lensing statistics. In this work we investigate two widely used estimators for the 2-point correlation function and power spectrum.

A. The standard estimator

The standard estimator [3, 23, 25] averages galaxy pairs in the lensing survey. For each galaxy cosmic shear is decomposed into the tangential shear $\gamma_{\rm t}$ and the cross component $\gamma_\times$ relative to the separation vector to the other galaxy in the pair. Then one calculates the following shear-shear correlation functions:

$$\xi_\pm(\theta) = \frac{\sum_{\alpha\beta}[\gamma_{{\rm t},\alpha}\gamma_{{\rm t},\beta} \pm \gamma_{\times,\alpha}\gamma_{\times,\beta}]w_\alpha w_\beta \Delta_{\alpha\beta}}{\sum_{\alpha\beta} w_\alpha w_\beta \Delta_{\alpha\beta}} \ , \qquad (5)$$

where galaxy pairs labeled α, β are separated by angular distance $\vartheta = |\vartheta_\alpha - \vartheta_\beta|$. $\Delta_{\alpha\beta} = 1$ counts for all the pairs with ϑ falling in the angular bin centered at θ, otherwise $\Delta_{\alpha\beta} = 0$. w_α is the weighting for each galaxy depending on some selection factors like the image quality, etc.. For brevity, we only discuss the simplified case $w_\alpha = 1$. Ideally (e.g. in the absence of SLC), these correlation functions are connected to the theory through the relationship

$$\xi_{+/-}(\theta) = \frac{1}{2\pi}\int_0^\infty {\rm d}\ell\ell J_{0/4}(\ell\theta) C_\kappa(\ell) \ , \qquad (6)$$

in which $J_{0/4}$ is the 0th- and 4th-order Bessel function of the first kind and $C_\kappa(\ell)$ is the power spectrum of weak lensing convergence. However, as shown above, the SLC effect is implicitly included through the summation over all galaxy pairs.

E-B decomposition is very useful in weak lensing analysis. B-modes are strong evidence for systematic errors, such as the point spread function [26], errors in shear estimation, galaxy intrinsic alignment, finite volume of the survey [27], and the SLC effect [21]. The E/B-mode power spectra can be obtained by

$$C_{E/B}(\ell) = \pi\int_0^\infty {\rm d}\theta\theta[J_0(\ell\theta)\xi_+(\theta) \pm J_4(\ell\theta)\xi_-(\theta)] \ . \qquad (7)$$

In simulations, the calculation of E/B-mode power spectrum can be simplified, without calculating $\xi_\pm$. First one measures the correlation functions

$$\hat{\xi}_{ij}(\vec{\theta}) = \frac{\langle(1+\delta_g^{\rm obs})\gamma_i(1+\delta_g'^{\rm obs})\gamma_j'\rangle}{\langle(1+\delta_g^{\rm obs})(1+\delta_g'^{\rm obs})\rangle} \ . \qquad (8)$$

Here $i, j = 1, 2$. The prime denotes for another line-of-sight (LoS). The denominator aveages over direction of $\vec{\theta}$. But the numerator does not. This allows us to do a 2D Fourier transform to obtain the corresponding 2D power spectrum $C_{ij}(\vec{\ell})$. We then aveage over the direction of $\vec{\ell}$ to obtain the E/B-mode power spectrum,

$$\begin{aligned} C_E(\ell) &= \langle C_{11}(\vec{\ell})\cos^2 2\varphi_{\vec{\ell}}\rangle + \langle C_{22}(\vec{\ell})\sin^2 2\varphi_{\vec{\ell}}\rangle \\ &\quad + \langle (C_{12}(\vec{\ell}) + C_{21}(\vec{\ell}))\cos 2\varphi_{\vec{\ell}}\sin 2\varphi_{\vec{\ell}}\rangle \ , \\ C_B(\ell) &= \langle C_{11}(\vec{\ell})\sin^2 2\varphi_{\vec{\ell}}\rangle + \langle C_{22}(\vec{\ell})\cos^2 2\varphi_{\vec{\ell}}\rangle \\ &\quad - \langle (C_{12}(\vec{\ell}) + C_{21}(\vec{\ell}))\cos 2\varphi_{\vec{\ell}}\sin 2\varphi_{\vec{\ell}}\rangle \ . \end{aligned} \qquad (9)$$

Here $\varphi_{\vec{\ell}}$ is the angle between the vector $\vec{\ell}$ and the x-axe in 2D Fourier space.

B. The pixel-based estimator

For the pixel-based estimator [23], one directly obtains an averaged cosmic shear γ from all galaxies in each pixel,

$$\hat{\gamma}_i = \frac{\int(1+\delta_g^{\rm obs})\gamma_i {\rm d}z}{\int(1+\delta_g^{\rm obs}){\rm d}z} \ . \qquad (10)$$

Here the integral (summation) is over all galaxies in the bin. Then we can construct lensing convergence map through

$$\kappa_E(\vec{\ell}) = \hat{\gamma}_1(\vec{\ell})\cos 2\varphi_{\vec{\ell}} + \hat{\gamma}_2(\vec{\ell})\sin 2\varphi_{\vec{\ell}} \ . \qquad (11)$$

The parity asymmetric B-mode convergence κ_B could be constructed as

$$\kappa_B(\vec{\ell}) = \hat{\gamma}_1(\vec{\ell})\sin 2\varphi_{\vec{\ell}} - \hat{\gamma}_2(\vec{\ell})\cos 2\varphi_{\vec{\ell}} \ . \qquad (12)$$

Then we could obtain E/B-mode power spectrum $C_{E/B}(\ell) = \langle\kappa_{E/B}(\vec{\ell})\kappa^*_{E/B}(\vec{\ell})\rangle$.

C. Different estimator, different SLC

The impact of SLC effect on these two estimators could be figured out in extreme cases.

For the standard estimator Eq. 8, if we have accurate redshift measurement and infinitesimal redshift bin size, the correlation between intrinsic source clustering and lens will be eliminated, $\langle\delta_g\delta_g'\gamma_i\gamma_j'\rangle \to \langle\delta_g\delta_g'\rangle\langle\gamma_i\gamma_j'\rangle$. Thus in this case the normalization will perfectly cancel the SLC induced by the intrinsic source clustering, $\hat{\xi}_{ij} \to \xi_{ij} \equiv \langle\gamma_i\gamma_j'\rangle$. However, in the context of lensing

tomography with photo-z measurement, there exists significant correlation between the source and lens (Fig. 1). The investigation in this paper will quantitively give us a conclusion about how large the SLC effect is and its dependence on redshift, scale and galaxy bias. For the cosmic magnification, $\delta_g^{\rm obs} = g\kappa$ always perfectly correlates with the lensing signal. Thus inevitably the standard estimator will suffer from the cosmic magnification. Adopting analytical analysis, the amplitude is expected to be proportional to $g\langle\kappa\gamma_i\gamma_j'\rangle/\langle\gamma_i\gamma_j'\rangle$.

For the pixel-based estimator Eq. 10, in the limit of constant $g\kappa$ across the photo-z bin, $\int(1+g\kappa)\gamma_i{\rm d}z \to (1+g\kappa)\int\gamma_i{\rm d}z$. Thus the normalization for each pixel will cancel the cosmic magnification induced SLC, leading to $\hat{\gamma}_i \to \gamma_i$ and $\hat{\xi}_{ij} \to \xi_{ij}$. The following investigation will tell us the SLC induced by the cosmic magnification is indeed negligible. However, the intrinsic source clustering is not a smooth function. Even worse, for low redshift the amplitude is not weak enough to make analytical analysis. Simulation is of great help to investigate this problem.

III. SIMULATION

Our N-body simulation was run using the Gadget-2 code [28] adopting the standard ΛCDM cosmology, with $\Omega_m = 0.266$, $\Omega_\Lambda = 1-\Omega_m$, $\sigma_8 = 0.801$, $h = 0.71$ and $n_s = 0.963$. The output redshifts are specified such that any two adjacent outputs are separated by the box size $L = 300h^{-1}$Mpc in comoving distance. More details can be found in [29]. All quantities involved in SLC effect (matter overdensity, convergence, cosmic shear) are constructed as follows.
(1) We stack 10 randomly shifted and rotated boxes to comoving distance $3000h^{-1}$Mpc. 20 light-cone realizations are made with sky coverage of $6.03^\circ \times 6.03^\circ$ each.
(2) We cut the light-cones into density slices $\delta_{m,i}$ ($i = 1,\cdots,140$) with $\Delta z = 0.01$, from $z = 0$ to $z = 1.4$, adopting NGP mass-assignment.
(3) We construct κ slices also with $\Delta z_s = 0.01$, according to

$$\kappa(\hat{n}, z_s) = \int_0^{\tilde{\chi}(z_s)} \delta_m(\hat{n}, z) W(z, z_s) {\rm d}\tilde{\chi} \qquad (13)$$

and the corresponding discrete form

$$\kappa_i(\hat{n}) = \sum_{j=1}^{i-1} \delta_{m,j}(\hat{n}) W_{ji} \Delta z \ . \qquad (14)$$

Here, δ_m is the matter overdensity. $\chi \equiv \chi(z)$ is the comoving angular diameter distance to the lens redshift z. We conveniently express χ in units of the Hubble radius, $\tilde{\chi} \equiv \chi/(c/H_0)$, in which H_0 is the Hubble constant today. The lensing kernel $W(z, z_s)$ for a source at redshift z_s and a lens at redshift z is given by

$$W(z, z_s) = \frac{3}{2}\Omega_m(1+z)\tilde{\chi}(z)\left[1 - \frac{\chi(z)}{\chi(z_s)}\right] \qquad (15)$$

when $z \le z_s$ and zero otherwise. The corresponding discrete form is

$$W_{ji} = \frac{3}{2}\Omega_m(1+z_j)\tilde{\chi_j}\left[1 - \frac{\chi_j}{\chi_i}\right] \ . \qquad (16)$$

Here Ω_m is the cosmological matter density of the universe in units of the critical density. The above expression is valid for the flat cosmology we consider throughout the paper.
(4) We convert κ slices into cosmic shear slices through the relation in Fourier space

$$\gamma_1(\vec{\ell}) = \kappa(\vec{\ell})\cos 2\varphi_{\vec{\ell}} \ , \qquad \gamma_2(\vec{\ell}) = \kappa(\vec{\ell})\sin 2\varphi_{\vec{\ell}} \ . \qquad (17)$$

A. For the Standard Estimator

For the standard estimator, we generate two sets of maps. One is

$$\gamma_{1,2}^{\delta_g}(\hat{n}) = \int_{z_{\rm min}}^{z_{\rm max}} \bar{n}_g(z_s)\gamma_{1,2}(\hat{n}, z_s)(1+\delta_g^{\rm obs}(\hat{n}, z_s)){\rm d}z_s \ . \qquad (18)$$

The superscript "δ_g" denotes that it is the product of cosmic shear and the source galaxy number denisty. The integeral is over the source redshift distribution. Numerically, we integrate over the range $z_{\rm min} < z < z_{\rm max}$, with $z_{\rm min} = z_{\rm min}^P - 0.2$ and $z_{\rm max} = z_{\rm max}^P + 0.2$ to take the broadening caused by photo-z errors into account (Fig. 2). $\bar{n}_g(z)$ is the real mean galaxy number density for the given photo-z bin and normalized to $\int\bar{n}_g(z_s){\rm d}z_s = 1$. The other map is the normalized galaxy surface number density,

$$\Sigma_g(\hat{n}) = \int_{z_{\rm min}}^{z_{\rm max}} \bar{n}_g(z_s)(1+\delta_g^{\rm obs}(\hat{n}, z_s)){\rm d}z_s \ . \qquad (19)$$

With the two maps, we can then calculate $\hat{\xi}_{ij}$ including the SLC effect through

$$\hat{\xi}_{ij}(\vec{\theta}) = \frac{\langle\gamma_i^{\delta_g}(\hat{n})\gamma_j^{\delta_g}(\hat{n}')\rangle}{\langle\Sigma_g(\hat{n})\Sigma_g(\hat{n}')\rangle}. \qquad (20)$$

The two lines of sight ($\hat{n}$,$\hat{n}'$) separates by $\vec{\theta}$. The denominator averages over all $\vec{\theta}$ falling in the given θ bin ($\theta - \Delta\theta/2 < |\vec{\theta}| < \theta + \Delta\theta/2$), but the numerator does not average over $\vec{\theta}$ in the bin. The above correlation functions are measured using FFT. Then we FFT $\hat{\xi}_{ij}(\vec{\theta})$ to obtain $C_{ij}(\vec{\ell})$ and then calculate the E/B-mode power spectrum using Eq. 9.

B. For the Pixel-based Estimator

For the pixel-based estimator, the averaged cosmic shear in the pixel centered at $\hat{n}$ is

$$\hat{\gamma}_{1,2}(\hat{n}) = \frac{\int_{z_{\rm min}}^{z_{\rm max}} \bar{n}_g(z_s)\gamma_{1,2}(\hat{n}, z_s)(1+\delta_g^{\rm obs}(\hat{n}, z_s)){\rm d}z_s}{\int_{z_{\rm min}}^{z_{\rm max}} \bar{n}_g(z_s)(1+\delta_g^{\rm obs}(\hat{n}, z_s)){\rm d}z_s} \ . \qquad (21)$$

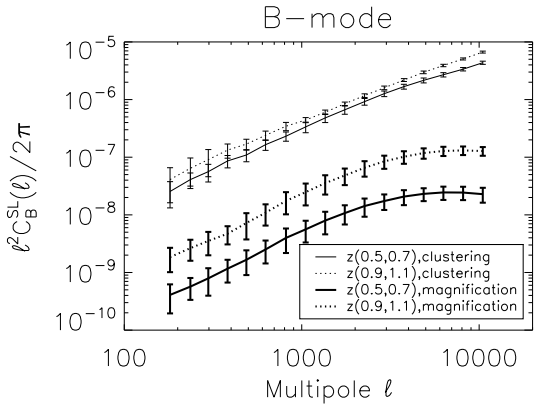

FIG. 3: SLC induced B-mode power spectrum in the standar estimator, for the case of intrinsic source clustering (thin lines) and cosmic magnification (thick lines). $b_g = 1$ and $g = 1$ are adopted. Solid and dotted lines are for photo-z bins $(0.5, 0.7)$ and $(0.9, 1.1)$, respectively. The error bars are the rms dispersion among 20 realizations. The B-mode is robustly identified in all cases.

Then we insert the above averaged cosmic shear into Eq. 11 & 12 to obtain the E/B-mode power spectrum.

We consider two typical photo-z bins $(0.5, 0, 7)$ and $(0.9, 1.1)$. This allows us to investigate the dependence of SLC on source redshift. We investigate two measures of SLC. (1) One is the B-mode power spectrum $C_B^{\rm SL}(\ell)$. Without SLC, the simulated cosmic shear has vanishing B-mode. So $C_B^{\rm SL}(\ell)$ provides a useful measure of SLC. (2) The other is the ratio of the E-mode power spectra in the presence and in the absence of SLC effect,

$$R(\ell) \equiv \frac{C_E^{\rm SL}(\ell)}{C_E(\ell)} \ . \tag{22}$$

We measure it for the two auto power spectra and one cross power spectrum between the two redshift bins.

We are also interested in the dependences of SLC on the galaxy bias b_g and the magnification bias factor g. Understanding these dependences helps calibrate the SLC effect. We choose $b_g = 0.5, 1, 1.5, 2$ and $g = -1, 1, 1.5, 2$ to study these dependences. We just substitute different b_g's and g's in $\delta_g^{\rm obs}(\hat{n}, z)$. To avoid unrealistic $\delta_g^{\rm obs}(\hat{n}, z) < -1$, which could happen if $b_g > 1$ or $g \gg 1$, we simply set $\delta_g^{\rm obs}(\hat{n}, z) = -1$ where it happens.

IV. SLC WITH THE STANDARD ESTIMATOR

This section presents our results on the impact of SLC on lensing power spectrum measured with the standard estimator.

A. Intrinsic Source Clustering

We take $\delta_g^{\rm obs} = \delta_g$ in Eq. 8 to quantify SLC effect due to the intrinsic source clustering. We assume $b_g = 1$ first.

1. B-mode power spectrum

The B-mode power spectrum is presented in Fig. 3, about 3 orders of magnitude lower than the E-mode. Despite its small value, the measurement of B-mode is robust, since its amplitude is 5 orders of magnitude larger than the case neglecting SLC effect (which is not presented here). The B-mode power spectrum is larger for higher photo-z bin $(0.9, 1.1)$. But this does not mean that the SLC effect is larger. Direct comparison of B-mode at the two redshifts is less meaningful, since the E-mode signal is also larger for higher redshift.

2. E-mode power spectrum

The impact of SLC on the E-mode auto- and cross-power spectrum, quantified by the ratio R (Eq. 22), is shown in Fig. 4. Although the measurement on R has large statistical uncertainty, we find $R > 1$. For $b_g = 1$, SLC amplifies the lensing E-mode power spectrum by 1-8% at $100 \lesssim \ell \lesssim 10^4$ for the photo-z bin $(0.5, 0.7)$. The impact becomes weaker at the higher photo-z bin $(0.9, 1.1)$. But its amplitude is still of the order 1% and hence non-negligible for precision weak lensing cosmology.

This overestimation of the E-mode lensing power spectrum by the standard estimator is caused by positive correlation between the lensing signal and the galaxy intrinsic clustering. From Eq. 8,

$$\hat{\xi}_{ij} - \xi_{ij} = \frac{\langle(\delta_g + \delta_g^{'})\gamma_i\gamma_j^{'}\rangle + \langle\delta_g\gamma_j^{'}\rangle\langle\delta_g^{'}\gamma_i\rangle + \langle\delta_g\gamma_i\delta_g^{'}\gamma_j^{'}\rangle_c}{1 + \langle\delta_g\delta_g^{'}\rangle} \ . \tag{23}$$

Since the intrinsic galaxy distribution is positively correlated with the lensing signal, the standard estimator overestimates the lensing power spectrum and we expect $R - 1 > 0$.

In contrast, the impact of SLC on the lensing cross-spectrum is much weaker and the measured $R-1$ is consistent with zero, within the error bars. For this case, we have

$$\hat{\xi}_{ij} - \xi_{ij} = \langle(\delta_g + \delta_g^{'})\gamma_i\gamma_j^{'}\rangle \ . \tag{24}$$

Hence we expect a weaker SLC effect. However, the above result shows that the SLC effect on cross-power spectrum is non-zero, although we lack the statistical accuracy to measure it.

To obtain the dependence on general values of b_g, we directly multiply the galaxy bias we choose on matter overdensity in the analysis, neglecting the evolution of

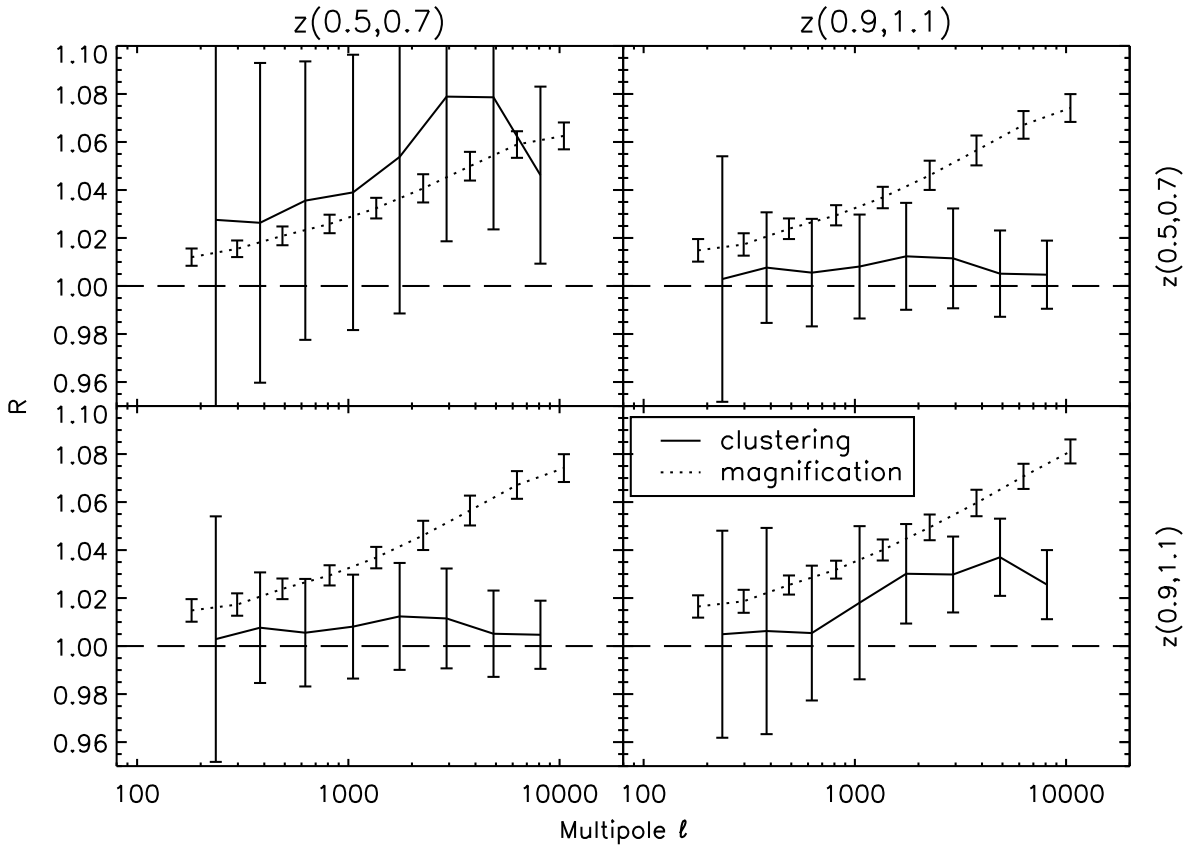

FIG. 4: The impact of SLC on the lensing auto- and cross-power spectrum measured by the standard estimator. We plot the ratio of the power spectra $R = C_E^{\rm SL}(\ell)/C_E(\ell)$, for $b_g = 1$ and $g = 1$, and for photo-z bins $(0.5, 0.7)$ and $(0.9, 1.1)$. The error bars are estimated from 20 realizations. SLC can bias the lensing E-mode power spectrum measurement by 1%-8% and the exact value depends on the galaxy bias (b_g) and the magnification prefactor (g).

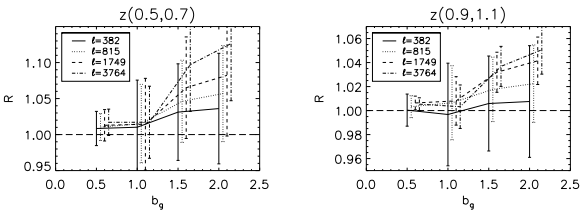

FIG. 5: The dependence of $R = C_E^{\rm SL}(\ell)/C_E(\ell)$ on b_g for standard estimator. The data points have $b_g = 0.5, 1, 1.5, 2$ respectively. For clarity, the results for different ℓ's are presented with arbitrary horizontal shifts. The dependence on galaxy bias is nonlinear.

bias across the redshift bin we consider. If the galaxy number density $\delta_g = b_g\delta_m < -1$, we just set it as -1 in this simple bias model. The results are shown in Fig. 5. The dependece on b_g is clearly nonlinear. This more complicated behavior is already implied by Eq. 23. From it, we have

$$R - 1 = \frac{b_g f_1(\ell) + b_g^2 f_2(\ell)}{1 + b_g^2 f_3(\ell)} \simeq b_g f_1 + b_g^2 f_2 - b_g^3 f_1 f_3 + \cdots , \tag{25}$$

in which f_1, f_2, f_3 are some functions of the underlying matter density δ_m and the lensing signal γ. Since the density fluctuation is of the order unity (Fig. 6), f_2 is comparable to f_1, leading to deviation from the linear dependence.

In principle we can fit the above results to obtain a fitting formula for the R-b_g relation. Such relation is useful to calibrate SLC in the standard estimator. b_g (up to a normalization) can be directly measured from the lensing survey. So by spliting source galaxies into flux bins (with different b_g), we can measure $C_E^{\rm SL}$-b_g relation and extrapolate to obtin C_E in the limit of $b_g = 0$. Unfortunately our simulation does not have sufficient independent realizations to beat down statistical fluctuations in R (Fig. 5), so we postpone more detailed investigation of R-b_g relation into future works.

We find that the standard estimator results in large cosmic variance in the power spectrum measurement

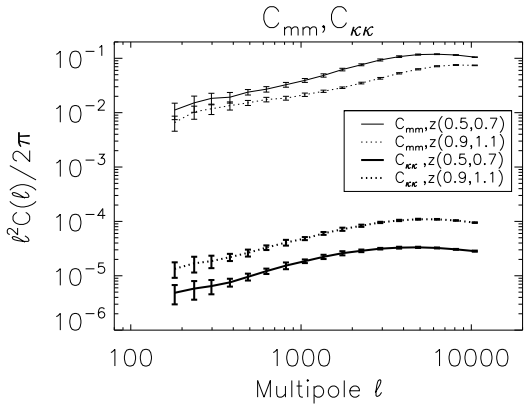

FIG. 6: The lensing power spectrum $C_{\kappa\kappa}$ and the galaxy angular power spectrum with $b_g = 1$ (C_{mm}) for photo-z bins $(0.5, 0.7)$ and $(0.9, 1.1)$. Large fluctuations in the galaxy distribution enhance statistical fluctuations in the lensing power spectrum measured by the standard estimator.

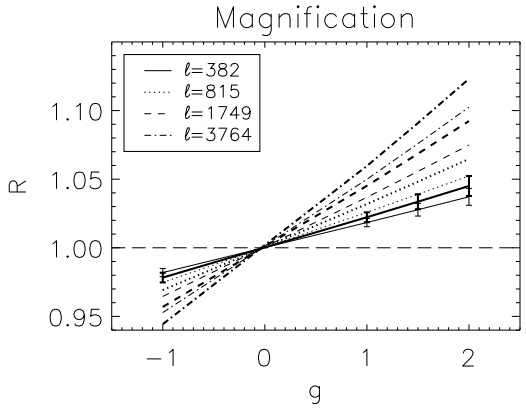

FIG. 7: The dependence of $R = C_E^{\rm SL}(\ell)/C_E(\ell)$ on g for standard estimator. Results are for photo-z bins $(0.5, 0.7)$ (thin lines) and $(0.9, 1.1)$ (thick lines). The data points have $g = -1, 1, 1.5, 2$, respectively. For clarity, we only plot the error bars for $\ell = 382$, which are the rms dispersion among 20 realizations. The dependence on g is perfectly linear.

(Fig. 4). For example, statistical fluctuation in R is $\sim 5\%$ for the photo-z bin $(0.5, 0.7)$ over the angular scale $100 \lesssim \ell \lesssim 10^4$. In particular, the cosmic variance does not decrease toward smaller angular scales, as we would expect. This is in sharp contrast with statistical fluctuation in the true E-mode lensing power spectrum or the angular galaxy power spectrum (Fig. 6).

We believe that this large cosmic variance is the result of modulation of the denominator $(1 + \xi_g)$ in the standard estimator (Eq. 8). Since the correlation between the lensing signal and the galaxy field is not strong, statistical fluctuation in the galaxy field ($\delta\xi_g$) is only partly eliminated in the standard estimator (Eq. 8). So it contributes to fluctuation in the measured lensing correlation function/power spectrum. Since the galaxy clustering is much stronger than the lensing signal ($C_{mm}/C_{\kappa\kappa} \sim 10^3$, Fig. 6), statistical fluctuation in the denominator can cause much larger (fractional) fluctuation in the measured lensing correlation function/power spectrum. This also explains the reduced error bars towards higher redshift, for the increasing magnitude of lensing signal and decreasing magnitude of ξ_g.

More careful analysis should be carried out against mock galaxy catalogue with galaxies of various types. Nevertheless, results here have robustly shown that SLC is non-negligible in the lensing correlation function/power spectrum measured through the standard estimator.

B. Cosmic Magnification

We take $\delta_g^{\rm obs} = g\kappa$ in Eq. 8 to quantify the SLC effect due to the cosmic magnification (magnification bias or size bias). We directly multiply the lensing convergence by the given g to obtain the map of $\delta_g^{\rm obs} = g\kappa$. In the analysis, we neglect the change of g across the redshift bin we consider. Unless for very bright galaxies in the exponential tail, this approximation is sufficiently accurate. Firstly we assume $g = 1$. We then try other values of g from -1 to 2.

1. B-mode power spectrum

The B-mode caused by the cosmic magnification induced SLC is robustly identified (Fig. 3). It is 2 orders of magnitude lower than the one due to the intrinsic source clustering and 5 orders of magnitude lower than the lensing E-mode. Hence it is too weak to detect in lensing surveys. However, this does not mean its impact on the E-mode lensing power spectrum is negligible. In contrast, its impact on the E-mode power spectrum is 4 orders of magnitude larger. As shown in Fig. 4, the SLC caused by this cosmic magnification affects the lensing E-mode power spectrum by a few percent. This is an example showing the danger of using B-mode as a diagnostic of lensing systematic errors.

2. E-mode power spectrum

SLC induced by the cosmic magnification has significant impact on the lensing E-mode power spectrum (Fig. 4). For example, at $\ell = 1000$ of particular interest in weak lensing cosmology, it enhances the lensing power spectrum by 3% for photo-z bin $(0.5, 0.7)$ and 4% for photo-z bin $(0.9, 1.1)$. The SLC effect on the cross-spectrum falles in between. The SLC effect also increases with ℓ, from 1% at $\ell \simeq 200$ to 6% at $\ell \simeq 10^4$, for the photo-z bin $(0.5, 0.7)$. These bebaviors can be roughly

understood as follows. From Eq. 8, we have (also refer to [23])

$$\hat{\xi}_{ij} - \xi_{ij} = \frac{2g\langle\kappa\gamma_i\gamma_j^{'}\rangle + g^2\langle\kappa\gamma_j^{'}\rangle\langle\kappa^{'}\gamma_i\rangle + g^2\langle\kappa\gamma_i\kappa^{'}\gamma_j^{'}\rangle_c}{1+g^2\xi_{\kappa\kappa}} \simeq 2g\langle\kappa\gamma_i\gamma_j^{'}\rangle \ . \quad (26)$$

The last expression has adopted the approximation $|\kappa| \ll 1$. The leading order correction $\langle\kappa\gamma\gamma\rangle$ grows faster than $\langle\kappa\kappa\rangle$ towards small scale and high redshift, so $R-1$ increases with both source redshift and ℓ (Fig. 4).

In contrast to the case of the intrinsic source clustering, R among realizations showes weaker fluctuations (Fig. 4). The reason is that statistical fluctuations in the denominator and the numerator of the standard estimator are strongly correlated and hence are largely cancelled out.

Eq. 26 predicts, for the auto-power spectrum,

$$R(\ell) - 1 = c(\ell)g \ . \quad (27)$$

Here $c(\ell)$ is determined by the ratio of lensing bispectrum and power spectrum, so it only depends on ℓ. This relation is confirmed to high accuracy in Fig. 7, where results for arbitrarily selected $g = -1, 1, 1.5, 2$ are presented. This linear relation holds for the two redshift bins and angular scales investigated ($\ell = 382, 815, 1749, 3764$). Notice that g could be zero or negative, leading to no correlation or anti-correlation between the source and lens.

For the cross correlation, we can derive a similar relation,

$$R(\ell) - 1 = c_f(\ell)g_f + c_b(\ell)g_b \ . \quad (28)$$

Here, g_f and g_b are the g factors of foreground and background galaxies. Again, $c_f(\ell)$ and $c_b(\ell)$ are determined by the ratio of lensing bispectrum and power spectrum for foreground and background, respectively. Note that g is also an observable in lensing survey. Thus if we further assign the source galaxies into different g-bins, according to the perfect scaling we could calibrate the SLC effect out. Furthermore, this calibration allow us to measure 3rd-order statistics ($\langle\gamma\gamma'\kappa'\rangle$ and $\langle\gamma\kappa\gamma'\rangle$) by comparing the power with SLC effect with the one calibrated.

C. Summary

From the results above, we summarize that the standard estimator suffers SLC effect induced by both the intrinsic source clustering and the cosmic magnification. Both of them cause $\mathcal{O}(1\%)$-$\mathcal{O}(10\%)$ overestimation in lensing power spectrum at angular scale and redshift of interest. The standard estimator also results in large cosmic variance in the power spectrum measurement. Such systematic error is significant for lensing cosmology. Fortunately, SLC induced by the cosmic magnification present a perfect linear dependence on observable g. So it is very promising to self-calibrate it using this linear relation. SLC induced by the intrinsic source clustering shows nonlinear dependence on b_g. However, in principle, through simulation we could obtain a useful fitting formula and self-calibrate it.

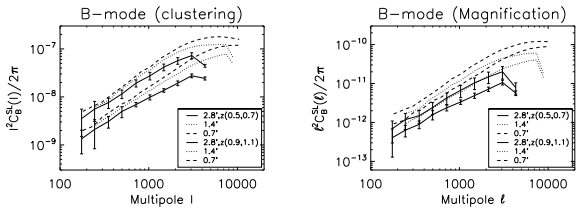

FIG. 8: The intrinsic source clustering (left panel) and cosmic magnification (right panel) induced B-mode power spectrum measured by the pixel-based estimator (with $b_g = 1$ and $g = 1$), for photo-z bins $(0.5, 0.7)$ (thin lines) and $(0.9, 1.1)$ (thick lines). 3 pixel sizes, $2.8'$, $1.4'$ and $0.7'$, are adopted. For clarity, we only plot the error bars for the pixel size of $2.8'$. The B-mode is robustly identified in all cases and the dependence on pixel size also shows up.

V. SLC WITH THE PIXEL-BASED ESTIMATOR

This section presents our results on the impact of SLC on lensing power spectrum measured with the pixel-based estimator. This estimator first obtains the averaged cosmic shear on each pixel of the sky and then uses this map to measure lensing statistics.

A. Intrinsic Source Clustering

We take $\delta_g^{\rm obs} = \delta_g$ in Eq. 10 to quantify the SLC effect due to the intrinsic source clustering, and look at $b_g = 1$ first. In general, all the results in this section depend on the pixel size. We show results with pixel size $0.7^{'}$, $1.4^{'}$ and $2.8^{'}$ to show this dependence. But for clarity, we only plot error bars for the $2.8'$ pixel size case.

1. B-mode power spectrum

The B-mode power spectrum is presented in the left panel of Fig. 8. A non-zero B-mode is detected at high significance. Furthermore, it is orders of magnitude higher than the case without SLC. Hence the B-mode caused by the intrinsic clustering induced SLC is robustly identified. It is slightly higher for lower photo-z bin $(0.5, 0.7)$, which is consistent with the E-mode result below. This should be due to stronger intrinsic clustering at lower redshift.

We also find smaller SLC effect for larger pixel size. Larger pixel suppresses the intrinsic clustering, leading to smaller SLC.

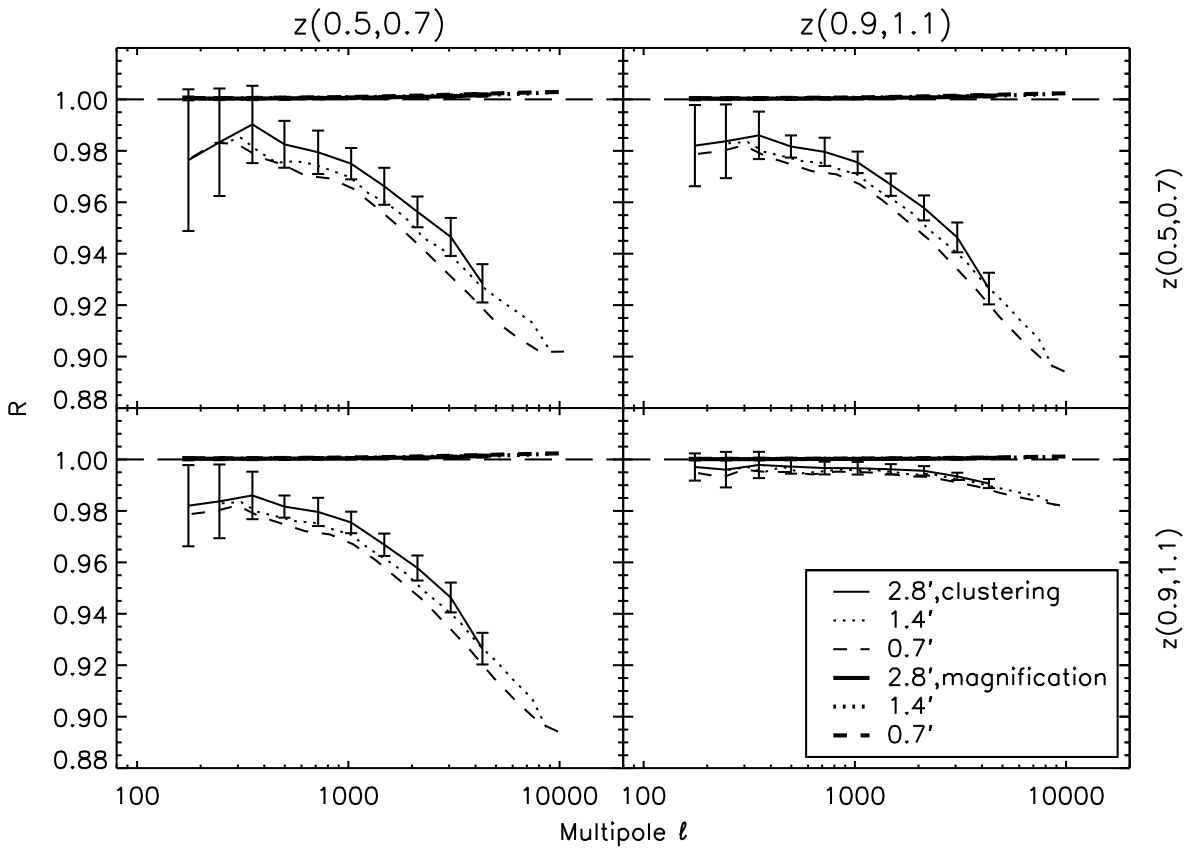

FIG. 9: The impact of SLC on the lensing power spectrum measured by the pixel-based estimator. We plot the ratio $R = C_E^{\rm SL}(\ell)/C_E(\ell)$, for different source redshift, different pixel size and different source of SLC. The pixel-based estimator overcorrects the SLC induced by the intrinsic source clustering, causing underestimation of the lensing power spectrum by $\sim 1\%$ at $\ell = 1000$ and $z_s \sim 1$. In contrast, it almost perfectly corrects the SLC induced by the cosmic magnification, leading to negligible bias in the measured lensing power spectrum.

2. E-mode power spectrum

The impact of SLC on the lensing power spectrum is shown in Fig. 9. An immediate finding is that it suppresses the E-mode power spectrum estimation. This arises from the fact that the intrinsic galaxy distribution (clustering, δ_g) is only weakly correlated with the lensing signal. So the pixel-based estimator (Eq. 10) overcorrects SLC, leading to underestimation of the lensing power spectrum. At $\ell \sim 1000$ of particular interest in weak lensing cosmology, this underestimation reaches 2% for the photo-z bin $(0.5, 0.7)$ and 1% for the photo-z bin $(0.9, 1.1)$. It increases towards small angular scale, where the intrinsic clustering is larger. This underestiamtion depends on the pixel size, except at scales much larger than the pixel size (e.g. the degree scale around $\ell = 200$).

A surprising result is that the cross-spectrum between the two photo-z bins is suppressed more than the auto-power spectrum of each bin. We argue that the source clustering of the two redshift bins biases the two lensing fields incoherently. Thus it largely reduces the coherence between the lensing signal at two redshifts and leads to larger suppression for cross-spectrum. This result is somewhat consistent with the result in [24], which found that SLC is important when cross-correlating low and high redshift bin.

The dependence of the detected underestimation on b_g is shown in Fig. 10. We find pretty good linearity for the high photo-z bin $(0.9, 1.1)$, and reasonably good for the low photo-z bin $(0.5, 0.7)$. Since our bias model is very simplified, further study against mock catalogue is required to robustly quantify R-b_g relation.

The detected 1% level bias in the measured lensing power spectrum is significant for precision lensing cosmology. Further analysis, including analysis against mock galaxy catalogue and analysis on PDF and peak statistics [30], should be carried out to fully understand the impact of SLC on weak lensing statistics based on the pixel-based estimator.

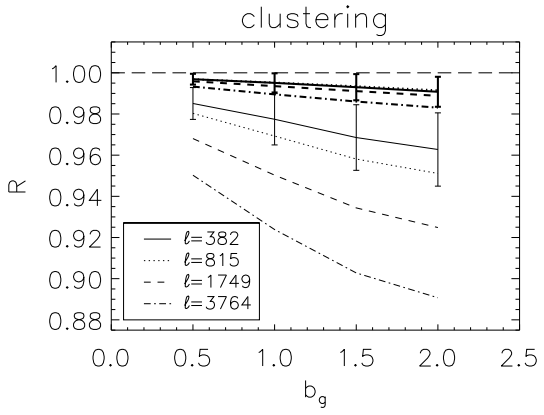

FIG. 10: The dependence of $R = C_E^{\rm SL}(\ell)/C_E(\ell)$ on the galaxy bias, for the pixel-based estimator. Results are for photo-z bins $(0.5, 0.7)$ (thin lines) and $(0.9, 1.1)$ (thick lines). For clarity, we only plot the errors for $\ell = 382$. The dependence on galaxy bias shows good linearity.

B. Cosmic Magnification

For the cosmic magnification induced SLC, we find that pixel-based estimator suppresses SLC to negligible level, both for the lensing B-mode (Fig. 8) and the E-mode (Fig. 9). This is valid for all the redshifts, pixel sizes and g investigated. The detected B-mode has a rms $\sim 10^{-5}$, orders of magnitude smaller than statistical fluctuations in cosmic shear measurement of full sky survey. So it is completely negligible. SLC affects the E-mode power spectrum by $\sim 0.1\%$ at $\ell \sim 1000$. This bias is again significantly smaller than the statistical accuracy of any realistic lensing surveys.

Why does the pixel-based estimator work so well? We argue that it is due to the fact that κ varies slowly across the photo-z bin, for each line of sight. In the limit that it can be well approximated as a constant along each line of sight, the weighting $1 + g\kappa$ in the numerator and denominator cancel out. So the averaged γ is area averaged, exactly what we want.

C. Summary

From the results above, we can conclude that the pixel-based estimator is essentially free of SLC induced by the cosmic magnification. So the SLC effect only arises from the intrinsic source clustering. It causes 1-10% underestimation of the lensing power spectrum at angular scale and redshift of interest. Such systematic error is significant for lensing cosmology. Fortunately we find that the induced SLC has a reasonably good linear dependence on the galaxy bias. So it is promising to self-calibrate the SLC effect using this linear relation.

VI. CONCLUSION AND DISCUSSION

We use N-body simulation to evaluate the SLC effect in the context of weak lensing tomography with realistic photo-z errors. We quantify the effect for two kinds of estimator, the standard estimator and the pixel-based estimator, and for two sources of the SLC effect, the intrinsic source clustering and the cosmic magnification. The statistics investigated include B-mode power spectrum, the ratio of E-mode power spectra, and the dependence on galaxy bias or magnification prefactor.

We found that in all cases, B-mode is clearly produced by the SLC effect. But the amplitude of the produced B-mode is at least 3 orders of magnitude lower than the E-mode. Thus these B-modes are not expected to be detected in near future lensing survey.

For the standard estimator, the SLC effect induced by both the source intrinsic clustering and the cosmic magnification can bias the lensing power spectrum by $\mathcal{O}(1\%)$-$\mathcal{O}(10\%)$ at the scale and redshift of interest. Furthermore, the standard estimator brings large cosmic variance into the power spectrum measurement. But the cross power spectrum suffers much less SLC effect induced by the source intrinsic clustering. These two sources of SLC together make the situation more complex. Fortunately, the SLC effect shows perfect linear dependence on observable g, which comes free from the lensing survey. Thus the self-calibration is very promising. Large sky coverage will beat down the fluctuations in the SLC effect induced by the intrinsic source clustering. When this uncertainty is well under control, in principle, we could find a fitting formula for the dependence on galaxy bias and apply it to the observation to self-calibrate the SLC effect induced by the source intrinsic clustering.

For the pixel-based estimator, we found negligible cosmic magnification induced SLC effect. However, the intrinsic source clustering induced SLC suppresses the power spectrum measurement by $\mathcal{O}(1\%)$-$\mathcal{O}(10\%)$. Fortunately, the dependence of SLC effect on galaxy bias shows good linearity. This linear scaling for low bias galaxies and for high redshift is also useful to self-calibrate the SLC effect.

From the result in this work, the pixel-based estimator has negligible SLC effect by the cosmic magnification. The source intrinsic clustering induced SLC effect shows good linear dependence on galaxy bias. Thus it is easy to deal with SLC effect by self-calibration. However, the standard estimator suffers sever SLC effect from both the two sources and large cosmic variance induced by the intrinsic source clustering. Although the dependence on g is perfectly linear, we need further works to deal with the SLC effect induced by the intrinsic source clustering.

For the standard estimator, the B-mode produced by intrinsic source clustering is consistent with the result in Schneider *et al.* [21] in which they analytically estimated the amplitude. We caution that lensing tomography indeed could suppress SLC effect induced by intrin-

sic source clustering, but not to a negligible level. The large SLC effect induced by cosmic magnification is consistent with the result in Schmidt *et al.* [23] in which they focused on lensing bias and analytically calculated the correction term from bispectrum. As pointed out in the literatures, the effect from approximating reduced shear as cosmic shear shares the same form with the cosmic magnification ($g = 1$). Our result is also consistent with the result for reduced shear in Dodelson *et al.* [12]. Thus our work here also confirms the result for reduced shear through simulation.

The SLC effect is a sever systematic in lensing cosmology. We need further investigations to deal with it. The bias in cosmological parameters is one important focus. The goodness of the above self-calibration method is also of great importance. We need more realistic lensing mock catalogue, with various types of galaxies, and more independent realizations to test these scaling relations and methods.

The standard estimator is convenient for the direct derivation of 2-point statistics from lensing survey. The pixel-based estimator is of great important for map-making and high order 1-point statistics. However, the underlying lensing signal is the same. Since the two estimators suffer differently from the SLC effect and have different dependence on galaxy bias and magnification prefactor, it is interesting to compare the measured lensing signal from the two. Due to the negligible SLC induced by the cosmic magnification and reasonably good R-b_g relation, it seems easier to get unbiased lensing signal from the pixel-based estimator. Combining this unbiased lensing signal with the one derived from the standard estimator, it is possible to identify the SLC effect in observation.

Acknowledgment

This work was supported by the national science foundation of China (Grant No. 11025316, 11121062, 10873027, 11233005, U1331201), the NAOC-Templeton beyond the horizon program, and the CAS/SAFEA International Partnership Program for Creative Research Teams (KJCX2-YW-T23). The work is also supported by the "Strategic Priority Research Program the Emergence of Cosmological Structures" of the Chinese Academy of Sciences, Grant No. XDB09010400.

[1] M. Bartelmann and P. Schneider, Phys. Rep. **340**, 291 (2001).
[2] A. Refregier, Annu. Rev. Astron. Astrophys. **41**, 645 (2003).
[3] D. Munshi, P. Valageas, L. van Waerbeke and A. Heavens, Phys. Rep. **462**, 67 (2008).
[4] H. Hoekstra and B. Jain, Annu. Rev. Nucl. Part. Sci. **58**, 99 (2008).
[5] M. Bartelmann, Class. Guantum Grav. **27**, 233001 (2010).
[6] LSST Dark Energy Science Collaboration, arXiv:1211.0310 (2012).
[7] D. Huterer, M. Takada, G. Bernstein and B. Jain, Mon. Not. R. Astron. Soc. **366**, 101 (2006).
[8] Y. Jing, Mon. Not. R. Astron. Soc. **335**, L89 (2002). C. M. Hirata and U. Seljak, Phys. Rev. D **70**, 063526 (2004). B. Jain, M. Jarvis and G. Bernstein, J. Cosmol. Astropart. Phys. **02**, 21 (2006). C. Heymans *et al.* , Mon. Not. R. Astron. Soc. **368**, 1323 (2006). C. Heymans, M. White, A. Heavens, C. Vale and L. van Waerbeke, Mon. Not. R. Astron. Soc. **371**, 750 (2006). L. van Waerbeke, M. White, H. Hoekstra and C. Heymans, Astropart. Phys. **26**, 91(2006). Z. Ma, W. Hu and D. Huterer, Astrophys. J. **636**, 21 (2006). S. Bridle and L. King, New J. Phys. **9**, 444 (2007). B. Joachimi and P. Schneider, Astron. Astrophys. **488**, 829 (2008). S. Bridle *et al.* , Ann. Appl. Stat., **3**, 6 (2009). T. Okumura and Y. Jing, Astrophys. J. **694**, L83 (2009). T. Okumura, Y. Jing and C. Li, Astrophys. J. **694**, 214 (2009). B. Joachimi and S. Bridle, Astron. Astrophys. **523**, 1 (2010). P. Zhang, Astrophys. J. **720**, 1090 (2010). P. Zhang, Mon. Not. R. Astron. Soc. **406**, L95 (2010). P. Zhang, U. Pen and G. Bernstein, Mon. Not. R. Astron. Soc. **405**, 359 (2010). G. Bernstein and D. Huterer, Mon. Not. R. Astron. Soc. **401**, 1399 (2010). J. Zhang and E. Komatsu, Mon. Not. R. Astron. Soc. **414** 1047 (2011). M. A. Troxel, M. Ishak, Mon. Not. R. Astron. Soc. **419**, 1804 (2012). M. A. Troxel, M. Ishak, Mon. Not. R. Astron. Soc. **423**, 1663 (2012). M. A. Troxel, M. Ishak, Mon. Not. R. Astron. Soc. **427**, 442 (2012). R. Mandelbaum *et al.* , arXiv:1308.4982 (2013).
[9] P. Schneider, L. van Waerbeke, B. Jain and G. Kruse, Mon. Not. R. Astron. Soc. **296**, 873 (1998).
[10] S. Dodelson, E. W. Kolb, S. Matarrese, A. Riotto and P. Zhang, Phys. Rev. D **72**, 103004 (2005).
[11] S. Dodelson and P. Zhang, Phys. Rev. D **72**, 083001 (2005).
[12] S. Dodelson, C. Shapiro and M. White, Phys. Rev. D **73**, 023009 (2006).
[13] M. White, Astropart. Phys. **22**, 211 (2004).
[14] H. Zhan and L. Knox, Astrophys. J. **616**, L75 (2004).
[15] Y. Jing, P. Zhang, W. Lin, L. Gao and V. Springel, Astrophys. J. **640**, L119 (2006).
[16] D. H. Rudd, A. R. Zentner and A. V. Kravtsov, Astrophys. J. **672**, 19 (2008).
[17] A.R. Zentner, D.H. Rudd and W. Hu, Phys. Rev. D **77**, 043507 (2008).
[18] F. Bernardeau, Astron. Astrophys. **338**, 375 (1998).
[19] T. Hamana, Mon. Not. R. Astron. Soc. **326**, 326 (2001).
[20] T. Hamana, S.T. Colombi, A. Thion, J.E.G.T. Devriendt, Y. Mellier and F. Bernardeau, Mon. Not. R. Astron. Soc. **330**, 365 (2002).
[21] P. Schneider, L. van Waerbeke and Y. Mellier, Astron. Astrophys. **389**, 729 (2002).
[22] J. E. Forero-Romero, J. Blaizot, J. Devriendt, L. V. Waerbeke and B. Guiderdoni, Mon. Not. R. Astron. Soc. **379**, 1507 (2007).

[23] F. Schmidt, E. Rozo, S. Dodelson, L. Hui and E. Sheldon, Astrophys. J. **702**, 593 (2009).
[24] P. Valageas, arXiv:1306.6151 (2013).
[25] C. Heymans *et al.* , Mon. Not. R. Astron. Soc. **427**, 146 (2012).
[26] H. Hoekstra, Mon. Not. R. Astron. Soc. **347**, 1337 (2004).
[27] M. Kilbinger, P. Schneider and T. Eifler, Astron. Astrophys. **457**, 15 (2006).
[28] V. Springel. Mon. Not. R. Astron. Soc. **364**, 1105 (2005).
[29] W. Cui, P. Zhang, and X. Yang, Phys. Rev. D **81**, 103528 (2010).
[30] J. Liu, Z. Haiman, L. Hui, J. M. Kratochvil, and M. May, arXiv:1310.7517 (2013).
[31] Dark Energy Survey, http://www.darkenergysurvey.org
[32] Large Synoptic Survey Telescope, http://www.lsst.org
[33] We should point out here that the correlation coefficient does not completely determine the strength of SLC. For example, it is invariant to a deterministic galaxy bias. But sources with stronger clustering (larger b_g) has larger SLC effect.